



# Highly Selenite-Tolerant Strain *Proteus mirabilis* QZB-2 Rapidly Reduces Selenite to Selenium Nanoparticles in the Cell Membrane

JinLan Huang, DaiHua Jiang\*, MingShi Wang and XueJiao Huang\*

Guangxi Colleges and Universities Key Laboratory of Crop Cultivation and Tillage, Guangxi University, Nanning, China

## OPEN ACCESS

### Edited by:

Qiaoyun Huang,  
Huazhong Agricultural University,  
China

### Reviewed by:

Judith Maria Braganca,  
Birla Institute of Technology  
and Science, India  
Ke-Qing Xiao,  
University of Leeds, United Kingdom

### \*Correspondence:

DaiHua Jiang  
dhjiang2008@gxu.edu.cn  
XueJiao Huang  
hxuejiao0412@sina.com

### Specialty section:

This article was submitted to  
Microbiotechnology,  
a section of the journal  
Frontiers in Microbiology

Received: 25 January 2022

Accepted: 14 March 2022

Published: 11 April 2022

### Citation:

Huang JL, Jiang DH, Wang MS  
and Huang XJ (2022) Highly  
Selenite-Tolerant Strain *Proteus  
mirabilis* QZB-2 Rapidly Reduces  
Selenite to Selenium Nanoparticles  
in the Cell Membrane.  
*Front. Microbiol.* 13:862130.  
doi: 10.3389/fmicb.2022.862130

The application of biosynthesized nano-selenium fertilizers to crops can improve their nutrient levels by increasing their selenium content. However, microorganisms with a high selenite tolerance and rapid reduction rate accompanied with the production of selenium nanoparticles (SeNPs) at the same time have seldom been reported. In this study, a bacterial strain showing high selenite resistance (up to 300 mM) was isolated from a lateritic red soil and identified as *Proteus mirabilis* QZB-2. This strain reduced nearly 100% of 1.0 and 2.0 mM selenite within 12 and 18 h, respectively, to produce SeNPs. QZB-2 isolate reduced  $\text{SeO}_3^{2-}$  to  $\text{Se}^0$  in the cell membrane with NADPH or NADH as electron donors.  $\text{Se}^0$  was then released outside of the cell, where it formed spherical SeNPs with an average hydrodynamic diameter of  $152.0 \pm 10.2$  nm. *P. mirabilis* QZB-2 could be used for SeNPs synthesis owing to its simultaneously high  $\text{SeO}_3^{2-}$  tolerance and rapid reduction rate.

**Keywords:** *Proteus mirabilis*, selenite reduction, membrane, selenium nanoparticles, reduction efficiency

## HIGHLIGHTS

- Microorganisms with a high selenite tolerance, selenite reduction capacity, and also the ability to produce selenium nanoparticles (SeNPs) have rarely been reported.
- Here, we report a *Proteus mirabilis* QZB-2 strain with a high selenite resistance (up to 300 mM).
- This strain exhibited excellent  $\text{SeO}_3^{2-}$  reduction efficiency, nearly exhausted all of the  $\text{SeO}_3^{2-}$  (1 or 2 mM) within 18 h and transformed  $\text{SeO}_3^{2-}$  into SeNPs more rapidly than any other bacteria reported to date.
- The  $\text{SeO}_3^{2-}$  reduction activity in QZB-2 cells was attributed to the cell membrane fraction, with or without NADH/NADPH serving as electron donors.
- Our results reveal that *P. mirabilis* QZB-2 is an attractive bacterial candidate for the synthesis of novel nano-Se fertilizers owing to its simultaneously high  $\text{SeO}_3^{2-}$  tolerance and rapid reduction rate.

## INTRODUCTION

Selenium (Se) is an essential trace nutrient for humans and plays an important role in maintaining body health and preventing diseases (Dinh et al., 2018; Yan et al., 2021). However, globally, 0.5–1 billion people suffer from Se deficiency (Li et al., 2021). The biofortification of crops with Se-rich fertilizers is considered to be the most effective way to increase human Se intake (Luo et al., 2019;

Zhang et al., 2019a; Li et al., 2021). While fertilizers can contain organic selenium and nano-selenium, selenite ( $\text{SeO}_3^{2-}$ ) and selenate ( $\text{SeO}_4^{2-}$ ) are the two major types of inorganic Se used in fertilizers because of their low cost. However, the utilization efficiency of selenite and selenate by plants is relatively low because of their high toxicity (Deng et al., 2017). Soluble nano-Se is less toxic than inorganic and organic Se and has a higher bioavailability (Zahedi et al., 2019; Kumar and Prasad, 2021). The application of nano-Se to foliage or soil can significantly enhance crop yield, quality, and Se content (Li et al., 2020, 2021). Thus, improving the processes for synthesizing of nano-Se fertilizers could enhance the development of Se-rich agricultural products.

Traditional physical and chemical methods to synthesize selenium nanoparticles (SeNPs) are costly and cause pollution. Therefore, biological approaches are generally preferred because they have a low-cost and are eco-friendly (Wang et al., 2018b; Kumar and Prasad, 2021). Studies have revealed that some bacterial strains, such as *Pseudomonas* spp. (Kuroda et al., 2011; Avendaño et al., 2016), *Bacillus* spp. (Blum et al., 1998; Oremland et al., 2004; Bao et al., 2016), *Clostridium* sp. (Bao et al., 2013), *Selenihalanaerobacter* sp. (Oremland et al., 2004), and *Sulfurospirillum* sp. (Oremland et al., 2004), can synthesize nano-Se. Most of them use  $\text{SeO}_3^{2-}$  as a raw material, but only a few can use both  $\text{SeO}_3^{2-}$  and  $\text{SeO}_4^{2-}$ . Moreover, most Se-reducing microorganisms have a limited tolerance to  $\text{SeO}_3^{2-}$  ( $\leq 100$  mM) and require 48 h or more to reduce all  $\text{SeO}_3^{2-}$  ( $\geq 1$  mM) to elemental selenium ( $\text{Se}^0$ ) (Table 1). Therefore, novel strains with high  $\text{SeO}_3^{2-}$  tolerance and robust  $\text{SeO}_3^{2-}$  reduction abilities are required to improve SeNP synthesis.

In this study, the aerobic bacterium *P. mirabilis* QZB-2, isolated from lateritic red soil in Guangxi, China, showed strong tolerance to high concentrations of  $\text{SeO}_3^{2-}$  (up to 300 mM). The QZB-2 strain reduced the majority of 1.0 and 2.0 mM  $\text{SeO}_3^{2-}$  to  $\text{Se}^0$  within 12 and 18 h, respectively. This reduction occurred in the cell membrane, after which  $\text{Se}^0$  was released outside the cell where it formed spherical SeNPs with an average hydrodynamic diameter of  $152.0 \pm 10.2$  nm. Our results reveal that *P. mirabilis* QZB-2 is a strong bacterial candidate for the synthesis of novel nano-Se fertilizers owing to its simultaneously high  $\text{SeO}_3^{2-}$  tolerance and rapid reduction rates.

## MATERIALS AND METHODS

### Culture Medium

Luria-Bertani (LB) medium (per liter, pH 7.0–7.2) was used for bacterial enrichment. It contained 5.00 g of yeast extract, 10.00 g of NaCl, and 10.00 g of tryptone per liter. A  $\text{Na}_2\text{SeO}_3$  solution was prepared in deionized water and sterilized by filtration.

### Isolation and Identification of Selenite-Reducing Bacteria

Soil samples were collected from a naturally occurring Se-rich lateritic red soil (0–15 cm depth) on dry land in Guangxi province, southern China ( $22^\circ 05' 31''$  N,  $108^\circ 32' 53''$  E). The total

Se in the soil was 0.53 mg/kg. To isolate Se-reducing bacteria, 1 g of the soil sample was suspended in 100 mL of sterilized LB broth supplemented with 1 mM  $\text{SeO}_3^{2-}$ , and cultured at  $30^\circ\text{C}$  (150 rpm) for 48 h. The bacterial strains were subcultured three times with an inoculum size of 5%. The culture solution was then diluted three times (from  $10^{-5}$  to  $10^{-7}$ ), and 100  $\mu\text{L}$  of each dilution was inoculated on LB agar plates containing 10.00 mM  $\text{SeO}_3^{2-}$ . The agar plates were incubated at  $30^\circ\text{C}$  for 24 h. Red colonies were continuously picked and subcultured onto new plate until the pure cultures were finally obtained. Of all the monocultures, the QZB-2 isolate was chosen for further experiments because of its high  $\text{SeO}_3^{2-}$  tolerance.

To identify the QZB-2 isolate, its cell morphology was determined using an Olympus BH-2 optical microscope. The antibiotic resistance of the QZB-2 strain was tested using 1 and 100  $\mu\text{g}/\text{mL}$  tetracycline, ampicillin, chloramphenicol, kanamycin, and gentamycin. Subsequently, the 16S rRNA gene was amplified using universal primers 27F (5'-AGAGTTTGATCMTGGCTCAG-3') and 1492R (5'-ACGTTACCT TGTTACGACTT-3') (Zhang et al., 2019b). The obtained sequence was compared with other previously published sequences of the bacterial 16S rRNA gene in the NCBI. Finally, a phylogenetic tree was constructed using MEGA 7.0 software (Huang et al., 2018b).

## Tolerance and Reduction of Selenite by the QZB-2 Strain

### Selenite Tolerance

The tolerance of the QZB-2 isolate to  $\text{SeO}_3^{2-}$  was assessed by determining the minimal inhibitory concentration (MIC) of  $\text{SeO}_3^{2-}$  (Huang et al., 2021). First, the QZB-2 strain was activated in an LB medium and then harvested at  $3,500 \times g$  for 5 min. The harvested cells were washed with a phosphate buffer (PBS) and inoculated into fresh LB medium supplemented with different concentrations of  $\text{SeO}_3^{2-}$  (0–600 mM). The culture was incubated at  $30^\circ\text{C}$  and 150 rpm for 24 h. Subsequently, 100  $\mu\text{L}$  of the culture cells was inoculated onto LB agar plates and incubated for an additional 72 h at  $30^\circ\text{C}$  to determine the  $\text{SeO}_3^{2-}$  concentration that inhibited the growth of the QZB-2 strain.

### Selenite Reduction

The activated QZB-2 strain was inoculated into an LB medium containing 1 or 2 mM  $\text{SeO}_3^{2-}$ . Two types of negative controls, without  $\text{SeO}_3^{2-}$  or without bacteria, were used. The cultures were incubated at  $30^\circ\text{C}$  on a shaker (150 rpm) for 36 h. The  $\text{SeO}_3^{2-}$  and  $\text{Se}^0$  contents, as well as the amount of bacterial growth, were determined every 6 h.

### Analytical Methods

Bacterial growth was determined based on the number of colony-forming units (CFUs), which was determined by spreading 100  $\mu\text{L}$  of the diluted culture on LB plates and incubating them at  $30^\circ\text{C}$  for 72 h.  $\text{SeO}_3^{2-}$  concentrations were determined using an atomic fluorescence morphology analyzer (SA-20; Jitian, Beijing), while  $\text{Se}^0$  content was measured using a spectrophotometric method, as described by Khoei et al. (2017).

**TABLE 1** | Some bacteria for reduction of selenium.

Bacteria	Tolerance of selenium		Reduction ability			References
	Se(IV)	Se(VI)	Starting selenium	Time	Reduction rate	
<i>Stenotrophomonas maltophilia</i>	—	—	0.5 mM Se(VI), 0.5 mM Se(IV)	48 h	99.8%, 81.2%	Dungan et al., 2003
<i>Citrobacter braakii</i>	—	—	2.3–3.2 µg/L Se(VI)	192 h	87–97%	Zhang and Frankenberger, 2006
<i>Bacillus</i> sp. RS1	—	—	1 mg/L Se(VI)	192 h	57%	Zhang and Frankenberger, 2007
<i>Bacillus</i> sp. STG-83	640 mM	320 mM	1 mM Se(VI), 1 mM Se(IV)	96 h	100%, 100%	Soudi et al., 2008
<i>Pseudomonas stutzeri</i> NT-1	94 mM	122 mM	0.9 mM Se(IV)	18 h	100%	Kuroda et al., 2011
<i>Clostridium</i> sp. BXM	—	—	1 mM Se(VI), 1 mM Se(IV)	360 h	36–49%	Bao et al., 2013
<i>Rhodopseudomonas palustris</i> N	8 mM	—	2 mM Se(IV)	192 h	82.00%	Li et al., 2014a
<i>Comamonas testosteroni</i> S44	100 mM	—	1 mM Se(IV)	24 h	40%	Zheng et al., 2014
<i>Shewanella oneidensis</i> MR-1	—	—	0.5 mM Se(IV)	12 h	82%	Li et al., 2014b
<i>Bacillus mycoides</i> SeITE01	—	—	2 mM Se(IV)	24 h	100%	Lampis et al., 2014
<i>Pseudomonas putida</i> KT2440	10 mM	—	1 mM Se(IV)	24 h	89%	Avendaño et al., 2016
<i>Bacillus oryzae</i> ZYK	—	—	1 mM Se(IV)	360	90%	Bao et al., 2016
<i>Stenotrophomonas maltophilia</i> SeITE02	—	—	2 mM Se(IV)	192 h	86%	Lampis et al., 2017
<i>Enterobacter cloacae</i> Z0206	—	—	2 mM Se(IV)	72 h	100%	Song et al., 2017
<i>Stenotrophomonas bentonitica</i> BII-R7	200 mM	—	2 mM Se(IV)	48 h	100%	Ruiz Fresneda et al., 2018
<i>Rahnella aquatilis</i> HX2	85 mM	590 mM	10 mM Se(VI), 5 mM Se(IV)	48 h	38.5%, 39.8%	Zhu et al., 2018
<i>Alcaligenes faecalis</i> Se03	120 mM	—	5 mM Se(IV)	48 h	100%	Wang et al., 2018a
<i>Proteus mirabilis</i> YC801	100 mM	—	1 mM Se(IV)	42 h	100%	Wang et al., 2018b
<i>Bacillus safensis</i> JG-B5T	—	—	2.5 mM Se(IV)	336 h	70%	Fischer et al., 2019
<i>Providencia rettgeri</i> HF16-A	100 mM	—	1 mM Se(IV)	42 h	100%	Huang et al., 2021

## Subcellular Localization of Selenite Reduction

Different fractions of QZB-2 were collected to determine the cell compartment where  $\text{SeO}_3^{2-}$  is reduced. First, QZB-2 isolate was incubated in an LB medium for 18 h (stationary phase) and centrifuged at  $10,000 \times g$  for 10 min at  $4^\circ\text{C}$ . The obtained bacterial cell pellets were washed twice with 0.9% NaCl and then treated with different reagents to extract the periplasmic, membrane, and cytoplasmic fractions, as reported by Khoei et al. (2017). Pellets were treated with lysozyme and EDTA for 10 min, then centrifuged at  $20,000 \times g$  for 30 min, after which the supernatant was collected as a periplasmic fraction. Subsequently, the pellets were resuspended in 50 mM NaCl and then disrupted by ultra-sonication for 15 min. The supernatant was harvested as a cytoplasmic fraction following the centrifugation of the suspension at  $20,000 \times g$  for 70 min. The membrane fraction was obtained after the pellet were resuspended in 50 mM phosphate-buffered saline (PBS) (pH 7.4).

To extract extracellular polymeric substance (EPS), QZB-2 isolate was incubated in an LB medium at  $30^\circ\text{C}$  for 5 day. Following this, the cultures were centrifuged at  $10,000 \times g$  for 30 min at  $4^\circ\text{C}$  to obtain the supernatant. After passing the supernatant through a  $0.45 \mu\text{m}$  filter, the supernatant was mixed with pre-cooled ethanol (1:1) and precipitated at  $-20^\circ\text{C}$  overnight. Finally, precipitated EPS was collected by centrifugation ( $10,000 \times g$ , 30 min,  $4^\circ\text{C}$ ) (Wang et al., 2018b). For supernatant preparation, the stationary phase cultures (18 h) were centrifuged at  $10,000 \times g$  for 10 min and  $4^\circ\text{C}$ , before the supernatant was passed through a  $0.22 \mu\text{m}$  filter and collected (Khoei et al., 2017).

Activity assays were conducted on a 96-well plate, where  $100 \mu\text{L}$  of intracellular and extracellular fractions were briefly added to each well that contained  $88 \mu\text{L}$  of PBS,  $10 \mu\text{L}$  of  $\text{SeO}_3^{2-}$  solution (2.0 mM), and  $2 \mu\text{L}$  of NADH or NADPH (electron donor, 2.0 mM). The plate was then cultivated at  $30^\circ\text{C}$  for 72 h. Plates without an electron donor, a cell fraction (the supernatant/cell protein/EPS), or  $\text{SeO}_3^{2-}$  were used as negative controls.

## Localization and Characterization of Selenium

QZB-2 isolate was cultured in an LB medium, either supplemented with 2 mM  $\text{SeO}_3^{2-}$  or without  $\text{SeO}_3^{2-}$ . After 24 h, the culture was centrifuged ( $5,000 \times g$  for 10 min) to collect bacterial cell pellets. For transmission electron microscopy (TEM) analysis, the pellet was fixed with 2.5% glutaraldehyde at  $4^\circ\text{C}$  for 24 h and dried in an ultra-low temperature freezer (ALPHAL-4LD PLUS, CHRIST Co., Germany) (Huang et al., 2021). For scanning electron microscopy-energy dispersive X-ray spectrometry (SEM-EDS), the pellet was fixed with 2.5% glutaraldehyde at  $4^\circ\text{C}$  for 24 h and then dehydrated in ethanol solutions (30, 50, 70, 90, and 100%) before drying.

## Analysis of Selenium Nanoparticles

First, the QZB-2 isolate was incubated in an LB medium containing 2 mM  $\text{SeO}_3^{2-}$  for 24 h and centrifuged at  $10,000 \times g$  for 10 min at  $4^\circ\text{C}$ . The resulting bacterial cell pellets were washed twice with 0.9% NaCl, resuspended in Tris-Cl buffer, and then disrupted by ultra-sonication. The SeNPs were harvested after the cell suspension was centrifuged at  $40,000 \times g$  for 40 min at  $4^\circ\text{C}$ .

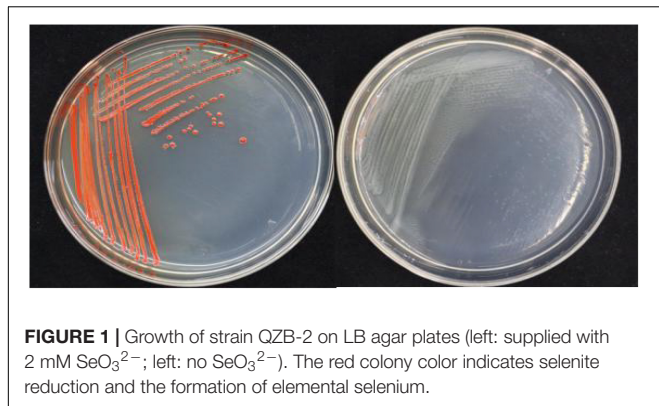


**FIGURE 1** | Growth of strain QZB-2 on LB agar plates (left: supplied with 2 mM SeO<sub>3</sub><sup>2-</sup>; left: no SeO<sub>3</sub><sup>2-</sup>). The red colony color indicates selenite reduction and the formation of elemental selenium.

Dynamic Light Scattering (DLS) and zeta potential analysis of SeNPs was conducted using a Nano-ZS90X Zeta potential particle size tester (Malvern, Britain) (Lampis et al., 2017). Afterward, the purified SeNPs were dried in an ultra-low temperature freezer (ALPHAL-4LD PLUS, CHRIST Co., Germany) for SEM-EDS, XRD, and FTIR analysis. Furthermore, the morphology and constituent elements analysis of SeNPs were analyzed using SEM-EDS. The compounds of SeNPs were analyzed using a D/Max-3C X-ray diffractometer with Cu-K radiation in the range of 10–80° (2θ) at a scan rate of 2°/min. The possible chemical bonds in SeNPs were investigated using a Fourier transformed infrared (FTIR) spectrophotometer in the range of 4,000–400 cm<sup>-1</sup> (Huang et al., 2018a).

### Statistical Analyses

The obtained data were analyzed by one-way analysis of variance (ANOVA) using SPSS Statistics 22 software. The level of statistical significance was set at *p* < 0.05. Graphics were plotted using Origin 8.6.

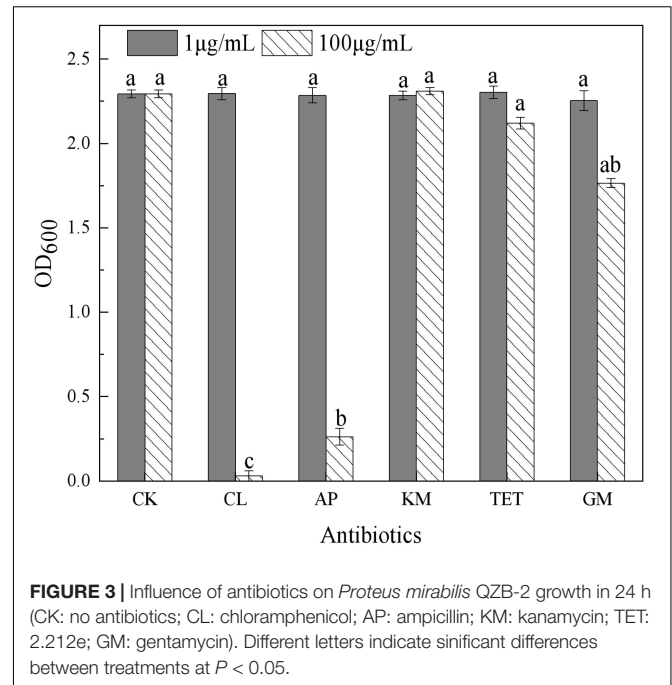


**FIGURE 3** | Influence of antibiotics on *Proteus mirabilis* QZB-2 growth in 24 h (CK: no antibiotics; CL: chloramphenicol; AP: ampicillin; KM: kanamycin; TET: 2.212e; GM: gentamycin). Different letters indicate significant differences between treatments at *P* < 0.05.

## RESULTS AND DISCUSSION

### Characterization and Identification of the QZB-2 Strain

In this study, 20 bacterial strains were isolated from naturally occurring Se-rich lateritic red soil in Guangxi, China, using LB plates supplemented with 20 mM SeO<sub>3</sub><sup>2-</sup>. Of these strains, the QZB-2 isolate was chosen for further experiments as it exhibited good growth and high SeO<sub>3</sub><sup>2-</sup> reduction ability

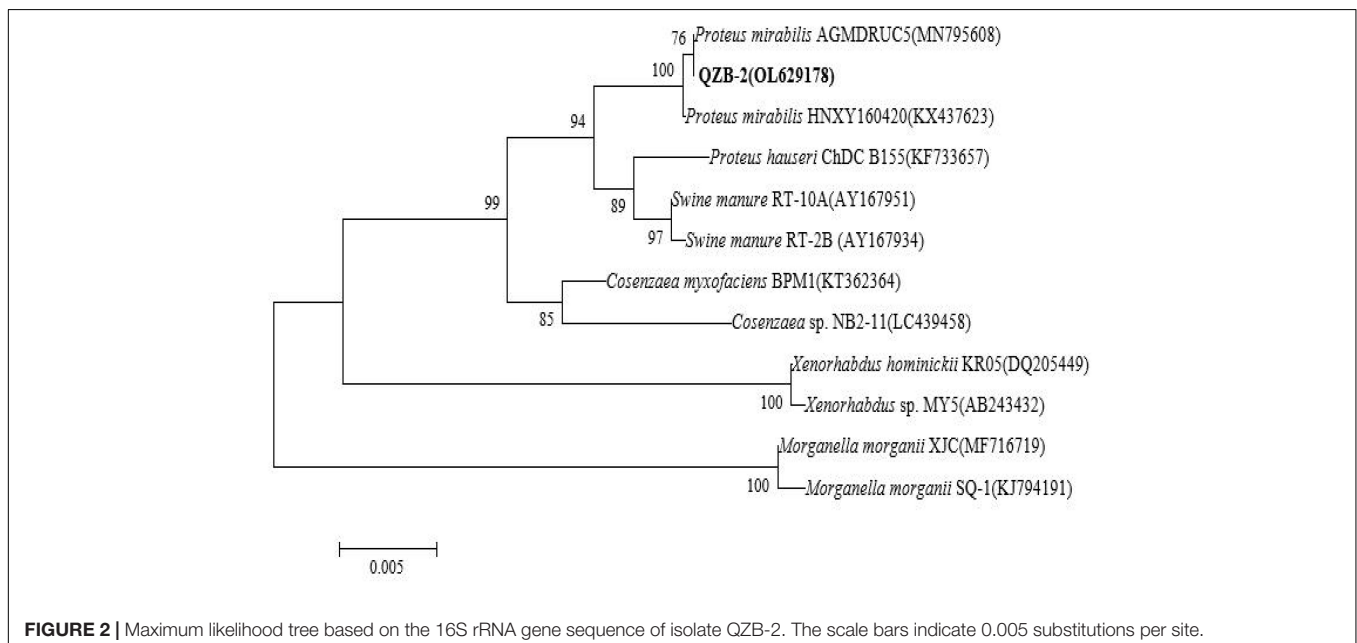


**FIGURE 2** | Maximum likelihood tree based on the 16S rRNA gene sequence of isolate QZB-2. The scale bars indicate 0.005 substitutions per site.

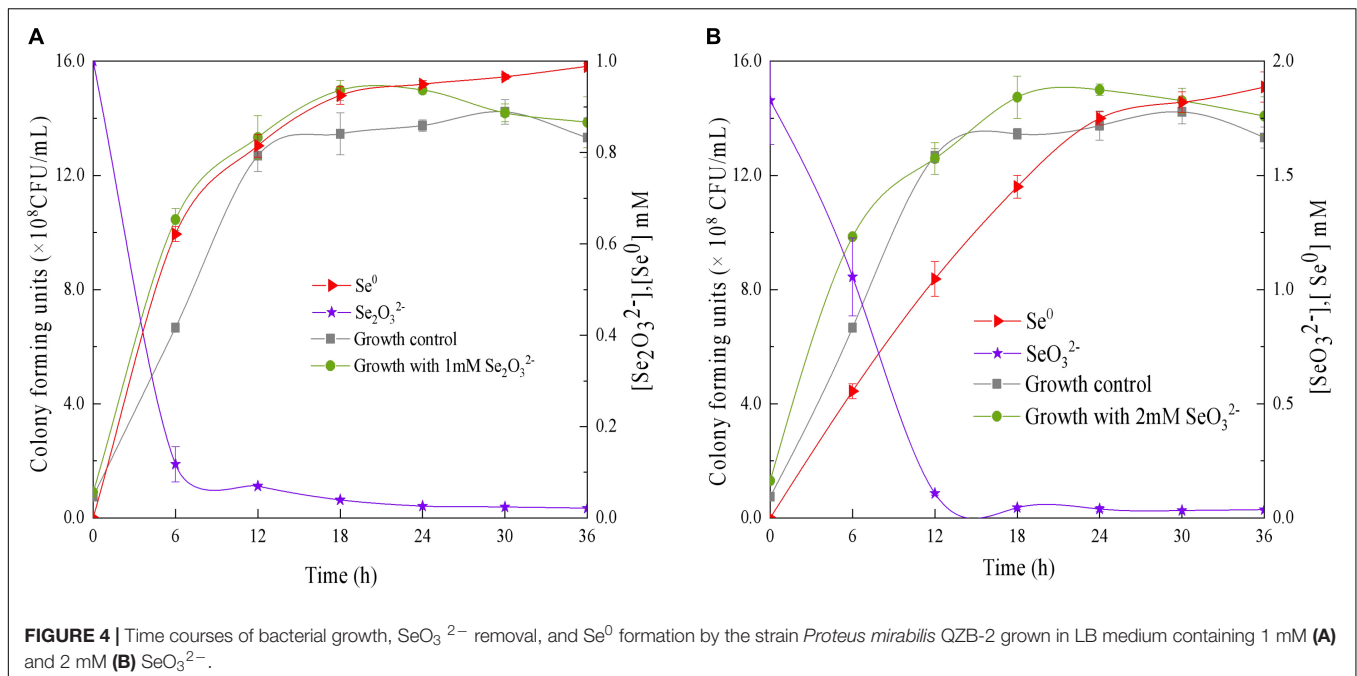
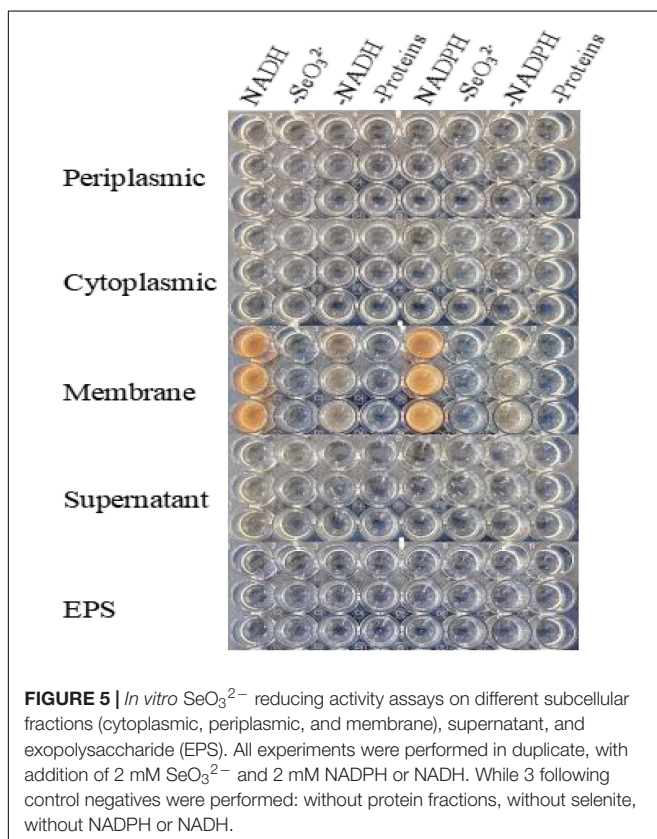


(Figure 1). Phylogenetic analysis indicated that the QZB-2 isolate was closely related to *P. mirabilis* AGMDRUC5 (MN795608) (Figure 2) and was therefore identified as *P. mirabilis* QZB-2

(OL629178). *Proteus* sp. is a rod-shaped gram-negative bacterium that is commonly found in the environment (Drzewiecka, 2016), with some strains exhibiting heavy metal ( $\text{Cr}^{6+}$ ,  $\text{Cu}^{2+}$ ,  $\text{Zn}^{2+}$ ) resistance (Rani et al., 2008; Ge et al., 2013; Islam et al., 2014). Recently, Wang et al. (2018a) reported that *P. mirabilis* YC801 isolated from insect guts could tolerate 100 mM  $\text{SeO}_3^{2-}$ . In this study, MIC assays showed that *P. mirabilis* QZB-2 could grow and produce  $\text{Se}^0$  even at a  $\text{SeO}_3^{2-}$  concentration of 300 mM (Figure 1). Moreover, *P. mirabilis* QZB-2 isolated from soil was resistant to several common antibiotics at concentrations from 1 to even 100  $\mu\text{g}/\text{mL}$  (Liu et al., 2021; Figure 3). Thus, we further explored the characteristics of  $\text{SeO}_3^{2-}$  reduction and SeNPs production in the QZB-2 strain.



### Selenite Reduction Characteristics by the QZB-2 Strain

The ability of QZB-2 to reduce  $\text{SeO}_3^{2-}$  was studied in liquid LB medium containing 1.0 or 2.0 mM of  $\text{SeO}_3^{2-}$ . Our results show that the relative growth curves of QZB-2 in a  $\text{SeO}_3^{2-}$  containing culture (both 1 and 2 mM) followed the same pattern as that in cultures without  $\text{SeO}_3^{2-}$  (Figure 4). These patterns confirmed that 1.0 and 2.0 mM of  $\text{SeO}_3^{2-}$  did not inhibit QZB-2 growth.  $\text{SeO}_3^{2-}$  depletion occurred at the start of the growth phase in the culture with 1.0 mM  $\text{SeO}_3^{2-}$  (Figure 4A). These findings are similar to those reported by Wang et al. (2018a), who found that  $\text{SeO}_3^{2-}$  was reduced by *P. mirabilis* YC801 after 6 h of incubation. However, *P. mirabilis* YC801 only reduced approximately 15% of the total  $\text{SeO}_3^{2-}$ , while the QZB-2 strain reduced the majority of the  $\text{SeO}_3^{2-}$  (88.0%) in 6 h (Figure 4). In most Se-reducing microorganisms,  $\text{SeO}_3^{2-}$  reduction occurs at the beginning or during the mid-exponential phase ( $\geq 12$  h) (Avenidaño et al., 2016; Lampis et al., 2017; Ruiz Fresneda et al., 2018). However, these

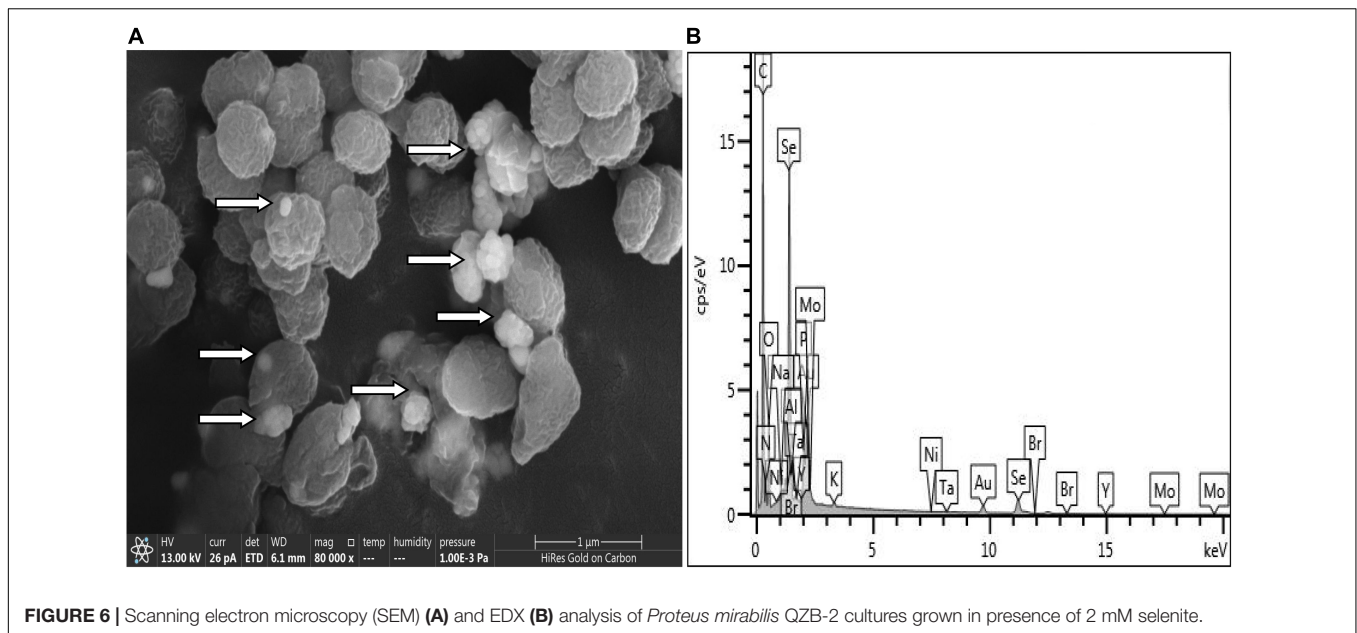


**FIGURE 6** | Scanning electron microscopy (SEM) (A) and EDX (B) analysis of *Proteus mirabilis* QZB-2 cultures grown in presence of 2 mM selenite.

microorganisms require more time (usually over 24 h) to reduce the majority of the  $\text{SeO}_3^{2-}$  (1 or 2 mM). In this study, the QZB-2 strain reduced both 1 and 2 mM of  $\text{SeO}_3^{2-}$  at the beginning of its growth and nearly exhausted all of the  $\text{SeO}_3^{2-}$  within 18 h. These results indicate that *P. mirabilis* QZB-2 has an excellent  $\text{SeO}_3^{2-}$  reduction efficiency.

In the QZB-2 strain,  $\text{SeO}_3^{2-}$  reduction was coupled with  $\text{Se}^0$  accumulation; after 6 h, 88% of the 1 mM  $\text{SeO}_3^{2-}$  was depleted while 70.45% of which was reduced to  $\text{Se}^0$  (Figure 4A). Conversely, a delay in  $\text{Se}^0$  formation has been observed in some bacteria, including *B. mycoides* SeITE01 (Lampis et al., 2014), *S. maltophilia* SeITE02 (Lampis et al., 2017), *A. faecalis* Se03 (Wang et al., 2018b), and *P. mirabilis* YC801 (Tugarova et al., 2018). We observed that in the QZB-2 strain more than 90% of the reduced  $\text{SeO}_3^{2-}$  (1 and 2 mM) was transformed into  $\text{Se}^0$  after 36 h of incubation (Figure 4). These results demonstrate that

*P. mirabilis* QZB-2 can tolerate high concentrations of  $\text{SeO}_3^{2-}$  and transforms  $\text{SeO}_3^{2-}$  into SeNPs more rapidly than any other bacteria reported to date.

### Subcellular Localization of Selenite Reduction

$\text{SeO}_3^{2-}$  reduction activity in the QZB-2 strain was localized in the cell membrane fraction (Figure 5), whereas in *A. faecalis* Se03, *P. mirabilis* YC801, and *P. rettgeri* HF16 cells, reduction activity is localized in the cytoplasmic fraction (Wang et al., 2018a,b; Huang et al., 2021). This shows that the  $\text{SeO}_3^{2-}$  reduction mechanism in QZB-2 is inconsistent with that observed in earlier studies.  $\text{SeO}_3^{2-}$  reduction in the QZB-2 strain only occurred when NADH or NADPH was present (Figure 5), which is consistent with reported  $\text{SeO}_3^{2-}$  reduction in *S. maltophilia* SeITE02 (Lampis et al., 2017) and *B. fungorum* strains (Khoie et al., 2017). Thus, we propose that  $\text{SeO}_3^{2-}$  reduction by *P. mirabilis* QZB-2 occurred in the cell membrane system through the catalytic activity of a reductase, with NADH/NADPH serving as electron donors. Moreover, SEM and EDX analysis show that SeNPs were found on the QZB-2 cell surface (Figures 6A,B), while TEM analysis illustrates that SeNPs were located in the extracellular space or cell membrane (Figure 7). Altogether, these findings suggest that the QZB-2 strain produced SeNPs within the cell and then released them into the medium.

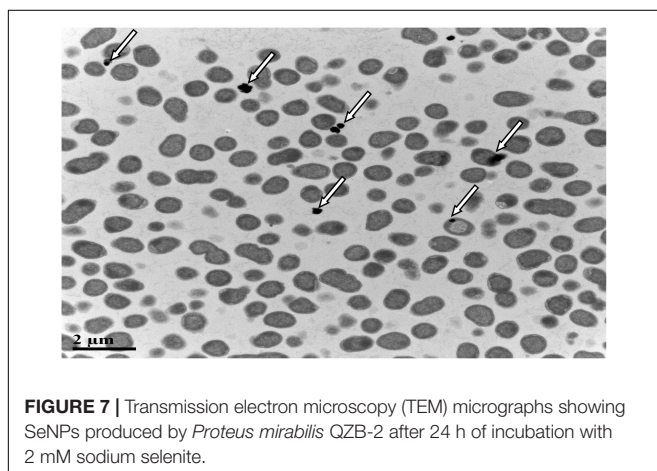


**FIGURE 7** | Transmission electron microscopy (TEM) micrographs showing SeNPs produced by *Proteus mirabilis* QZB-2 after 24 h of incubation with 2 mM sodium selenite.

### Characterization of Selenium Nanoparticles

Results of DLS analysis of the purified SeNPs are presented in Figures 8A,B. They had an average hydrodynamic diameter of  $152.0 \pm 10.2$  nm (Figures 8B,C). Moreover, the existence of Se was determined by EDX analysis, with selenium-specific peaks observed at 1.38 and 11.22 keV (Figure 8D), and

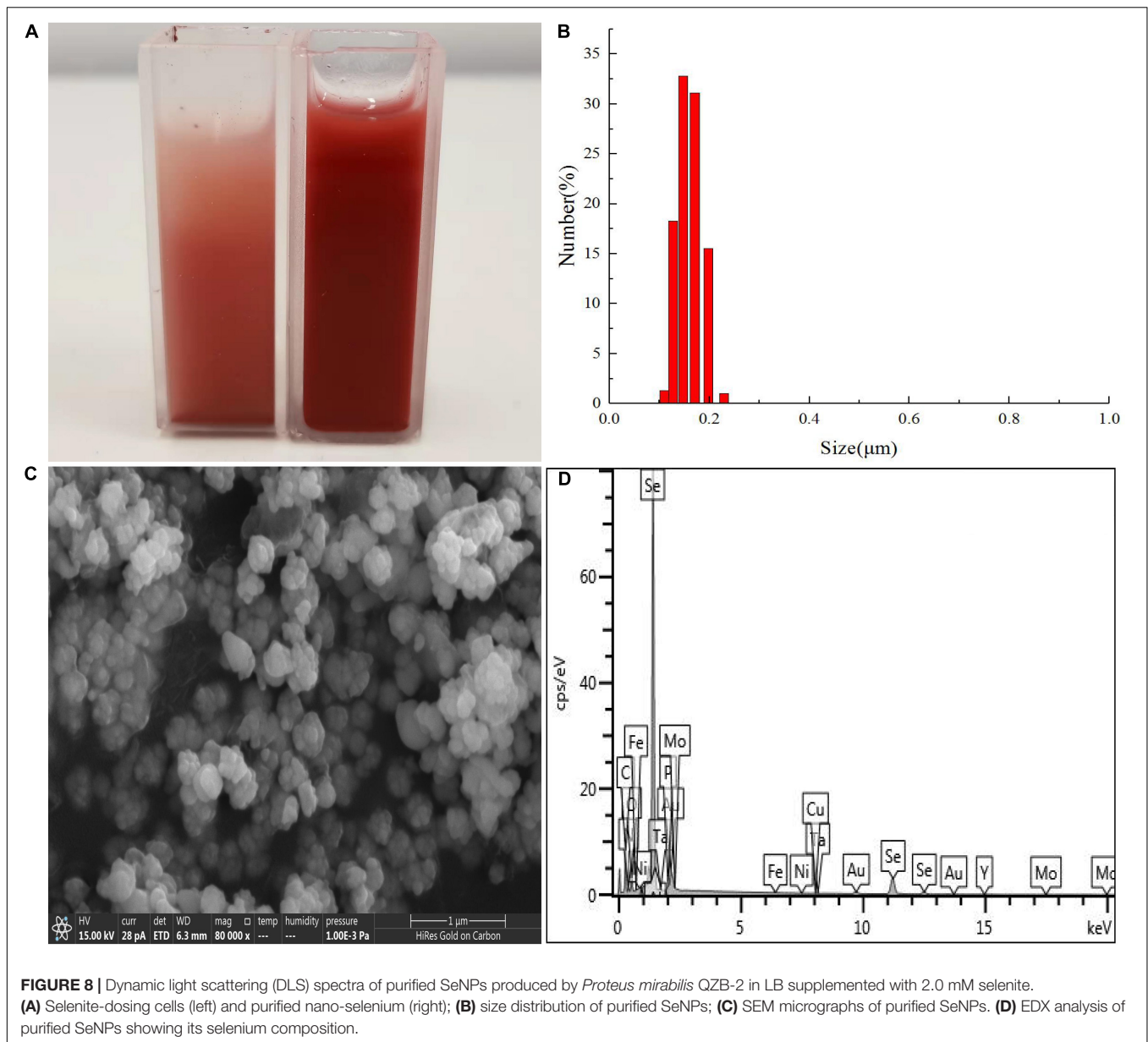
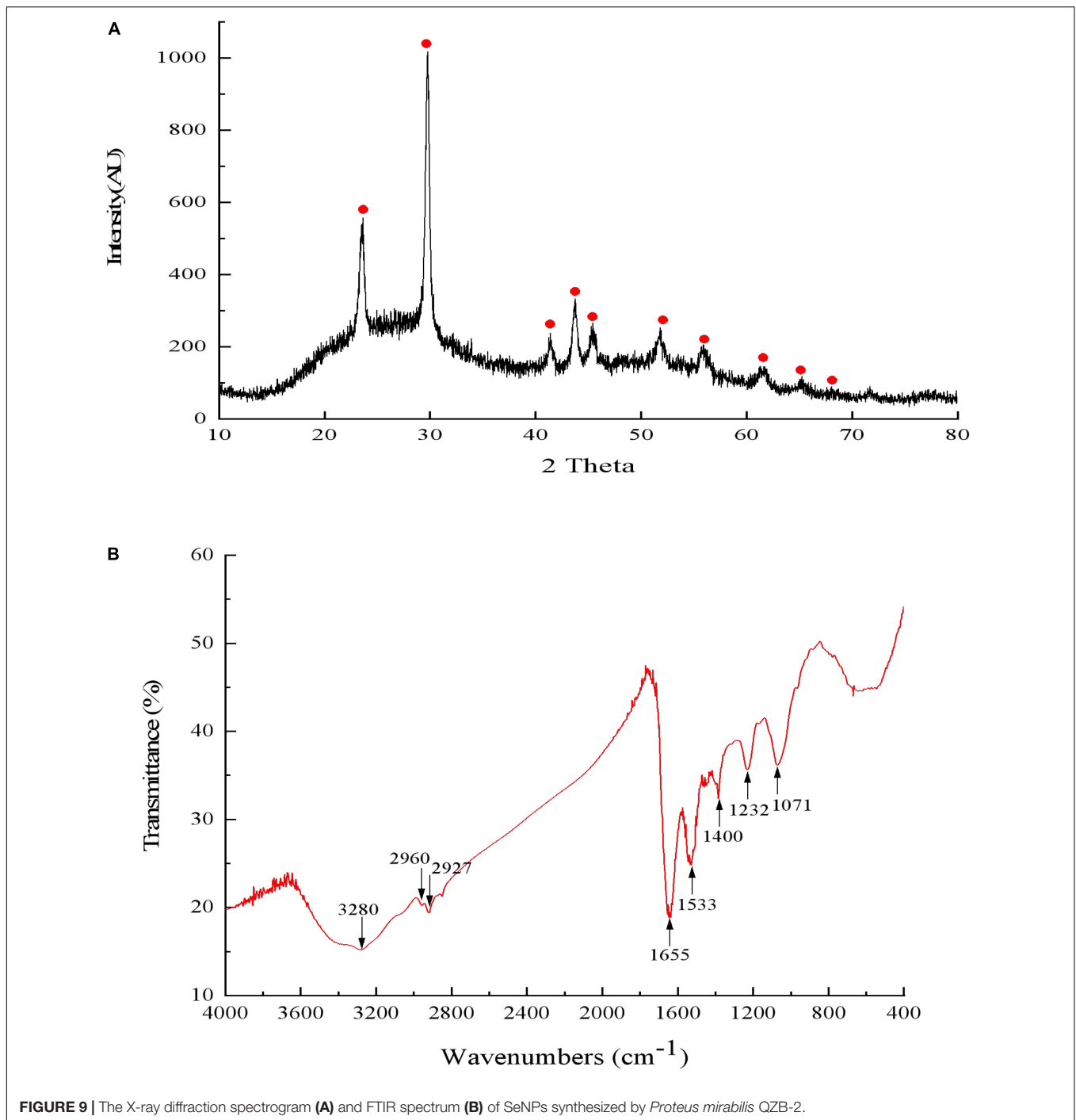


**Figure 9A** shows the XRD traces of SeNPs. The diffraction peaks at  $2\theta = 23.6, 29.7, 41.3, 43.7, 45.4, 51.9, 56.3, 61.9, 65.2,$  and  $68.6^\circ$  indicated the presence of the pure selenium in the sample (Shin et al., 2007). In addition, the FTIR spectra of the SeNPs are shown in **Figure 9B**. The absorption band at  $3,280\text{ cm}^{-1}$  is due to the stretching vibration of protein-modified N-H, amide A, or amide II (Zonaro et al., 2017; Wang et al., 2018b). The weak absorption peaks at  $2,960$  and  $2,927\text{ cm}^{-1}$  represent the symmetric stretching vibrations of C-H in the sugar ring or peptide chain (Xu et al., 2018). The peaks at  $1,655, 1,533,$  and  $1,232\text{ cm}^{-1}$  are accompanied by a low-intensity band and represent amide I, amide II, and amide III, respectively, which is a typical protein pattern (Kamnev et al., 2017; Wang et al., 2018b). The peak at  $1,400\text{ cm}^{-1}$  is because of the symmetric stretching vibration of carboxylate

(COO<sup>-</sup>), while its asymmetric counterpart can be seen at  $1,655\text{ cm}^{-1}$  (Lampis et al., 2017; Zonaro et al., 2017; Wang et al., 2018b). The bands at  $1,071\text{ cm}^{-1}$  are typical of C-O vibrations in carbohydrates, which may suggest the existence of polysaccharides (Tugarova et al., 2018; Wang et al., 2018b). The results of FTIR analysis clearly show that the surface of the SeNPs produced by *P. mirabilis* QZB-2 contained organic residues from carbohydrates, lipids, and proteins. The composition of these organic groups was in accordance with those produced by *S. maltophilia* SeITE02 and *P. mirabilis* YC801 (Lampis et al., 2017; Wang et al., 2018a). These organic groups could participate in  $\text{SeO}_3^{2-}$  reduction, as well as SeNP formation and stabilization processes.

A previous study showed that selenite and selenate were not suitable additives when applied as plant growth fertilizers



owing to their high toxicity (Deng et al., 2017). However, when using as a fertilizer, nano-Se could significantly enhance the Se content of crops (Li et al., 2020, 2021), which can safely increase human Se intake. Our study found that strain QZB-2 could tolerate high level of  $\text{SeO}_3^{2-}$ ; it rapidly reduces  $\text{SeO}_3^{2-}$  to  $\text{Se}^0$  while simultaneously synthesizing SeNPs. This result indicates strain QZB-2 could be used for SeNPs synthesis. However, the application of these synthesized nanoparticles in fertilizer has not been well-characterized and requires further study.

## CONCLUSION

The highly selenite-tolerant (up to 300 mM) strain *P. mirabilis* QZB-2 was isolated from a naturally occurring Se-rich paddy soil. QZB-2 reduced almost all selenite to form selenium nanoparticles within 18 h. The  $\text{SeO}_3^{2-}$  reduction activity in QZB-2 cells was attributed to the cell membrane fraction with NADH/NADPH serving as electron donors. Therefore, the QZB-2 bacterial strain is a promising candidate for the production of

novel nano-selenium fertilizers owing to its simultaneously high  $\text{SeO}_3^{2-}$  tolerance and rapid reduction rate.

## DATA AVAILABILITY STATEMENT

The original contributions presented in the study are publicly available. This data can be found here: OL629178.

## AUTHOR CONTRIBUTIONS

XH and DJ: conceptualization, writing—review and editing, and funding acquisition. JH: methodology, data curation, visualization, supervision, and writing—original draft preparation. MW: software, formal analysis, and investigation.

## REFERENCES

- Avedaño, R., Chaves, N., Fuentes, P., Sánchez, E., Jiménez, J. I., and Chavarría, M. (2016). Production of selenium nanoparticles in *Pseudomonas putida* KT2440. *Sci. Rep.* 6:37155. doi: 10.1038/srep37155
- Bao, P., Huang, H., Hu, Z. Y., Häggblom, M. M., and Zhu, Y. G. (2013). Impact of temperature, CO<sub>2</sub> fixation and nitrate reduction on selenium reduction, by a paddy soil *Clostridium* strain. *J. Appl. Microbiol.* 114, 703–712. doi: 10.1111/jam.12084
- Bao, P., Xiao, K. Q., Wang, H. J., Xu, H., Xu, P. P., Jia, Y., et al. (2016). Characterization and potential applications of a selenium nanoparticle producing and nitrate reducing bacterium *Bacillus oryziterrae* sp. nov. *Sci. Rep.-U.K* 6:34054. doi: 10.1038/srep34054
- Blum, J. S., Bindi, A. B., Buzzelli, J., Stolz, J. F., and Oremland, R. S. (1998). *Bacillus arsenicoselenatis*, sp. nov. and *Bacillus selenitireducens*, sp. nov.: two haloalkaliphiles from mono lake, California that respire oxyanions of selenium and arsenic. *Arch. Microbiol.* 171, 19–30. doi: 10.1007/s002030050673
- Deng, X. F., Liu, K. Z., Li, M. F., Zhang, W., Zhao, X. H., Zhao, Z. Q., et al. (2017). Difference of selenium uptake and distribution in the plant and selenium form in the grains of rice with foliar spray of selenite or selenate at different stages. *Field Crops Res.* 211, 165–171. doi: 10.1016/j.fcr.2017.06.008
- Dinh, Q. T., Cui, Z. W., Huang, J., Tran, T. A. T., Wang, D., Yang, W. X., et al. (2018). Selenium distribution in the Chinese environment and its relationship with human health: a review. *Environ. Int.* 112, 294–309. doi: 10.1016/j.envint.2017.12.035
- Drzewiecka, D. (2016). Significance and roles of proteus spp. bacteria in natural environments. *Microb. Ecol.* 72, 741–758. doi: 10.1007/s00248-015-0720-6
- Dungan, R., Yates, S., and Frankenberger, W. (2003). Transformation of selenate and selenite by *Stenophomonas maltophilia* isolated from a seleniferous agricultural drainage pond sediment. *Environ. Microbiol.* 5, 287–295. doi: 10.1046/j.1462-2920.2003.00410.x
- Fischer, S., Krause, T., Lederer, F., Mohamed, M., Shevchenko, A., Hübner, R., et al. (2019). *Bacillus safensis* JG-B5T affects the fate of selenium by extracellular production of colloidal less stable selenium nanoparticles. *J. Hazard. Mater.* 384, 121–146. doi: 10.1016/j.jhazmat.2019.12.1146
- Ge, S. M., Dong, X. J., Zhou, J. M., and Ge, S. C. (2013). Comparative evaluations on bio-treatment of hexavalent chromate by resting cells of *Pseudochromobacter* sp. and *Proteus* sp. in wastewater. *J. Environ. Manage.* 126, 7–12. doi: 10.1016/j.jenvman.2013.04.011
- Huang, S. W., Wang, Y. T., Tang, C. G., Jia, H. L., and Wu, L. F. (2021). Speeding up selenite bioremediation using the highly selenite-tolerant strain *Providencia rettgeri* HF16-A novel mechanism of selenite reduction based on proteomic analysis. *J. Hazard. Mater.* 406:124690. doi: 10.1016/j.jhazmat.2020.124690
- Huang, X. J., Ni, J. P., Yang, C., Feng, M., Li, Z. L., and Xie, D. T. (2018b). Efficient ammonium removal by bacteria *RhodoPseudomonas* isolated from natural landscape water: China case study. *Water* 10:1107. doi: 10.3390/w10081107

XH, MW, and DJ: validation. XH: resources and project administration. All authors have read and agreed to the published version of the manuscript.

## FUNDING

This work was supported by the National Natural Science Foundation of China (41661076 and 42107333).

## SUPPLEMENTARY MATERIAL

The Supplementary Material for this article can be found online at: <https://www.frontiersin.org/articles/10.3389/fmicb.2022.862130/full#supplementary-material>

- Huang, X. J., Feng, M., Ni, C. S., Xie, D. T., and Li, Z. L. (2018a). Enhancement of nitrogen and phosphorus removal in landscape water using polymeric ferric sulfate as well as the synergistic effect of four kinds of natural rocks as promoter. *Environ. Sci. Pollut. Re.* 25, 12859–12867. doi: 10.1007/s11356-018-1553-x
- Islam, F., Yasmeen, T., Riaz, M., Arif, M. S., Ali, S., and Raza, S. H. (2014). *Proteus mirabilis* alleviates zinc toxicity by preventing oxidative stress in maize (*Zea mays*) plants. *Ecotoxicol. Environ. Saf.* 110, 143–152. doi: 10.1016/j.ecoenv.2014.08.020
- Kamnev, A. A., Mamchenkova, P. V., Dyatlova, Y. A., and Tugarova, A. V. (2017). FTIR spectroscopic studies of selenite reduction by cells of the rhizobacterium *Azospirillum brasilense* Sp7 and the formation of selenium nanoparticles. *J. Mol. Struct.* 1140, 106–112. doi: 10.1016/j.molstruc.2016.12.003
- Khoei, N. S., Lampis, S., Zonaro, E., Yrjälä, K., Bernardi, P., and Vallini, G. (2017). Insights into selenite reduction and biogenesis of elemental selenium nanoparticles by two environmental isolates of *Burkholderia fungorum*. *New Biotechnol.* 34, 1–11. doi: 10.1016/j.nbt.2016.10.002
- Kumar, A., and Prasad, K. S. (2021). Role of nano-selenium in health and environment. *J. Biotechnol.* 325, 152–163. doi: 10.1016/j.jbiotec.2020.11.004
- Kuroda, M., Notaguchi, E., Sato, A., Yoshioka, M., Hasegawa, A., Kagami, T., et al. (2011). Characterization of *Pseudomonas stutzeri* NT-I capable of removing soluble selenium from the aqueous phase under aerobic conditions. *J. Biosci. Bioeng.* 112, 259–264. doi: 10.1016/j.jbiosc.2011.05.012
- Lampis, S., Zonaro, E., Bertolini, C., Bernardi, P., Butler, C. S., and Vallini, G. (2014). Delayed formation of zero-valent selenium nanoparticles by *Bacillus mycoides* SeITE01 as a consequence of selenite reduction under aerobic conditions. *Microb. Cell Factories* 13, 1–14. doi: 10.1186/1475-2859-13-35
- Lampis, S., Zonaro, E., Bertolini, C., Ceconi, D., Monti, F., Micaroni, M., et al. (2017). Selenite biotransformation and detoxification by *Stenotrophomonas maltophilia* SeITE02: novel clues on the route to bacterial biogenesis of selenium nanoparticles. *J. Hazard. Mater.* 324, 3–14. doi: 10.1016/j.jhazmat.2016.02.035
- Li, B. Z., Liu, N., Li, Y. Q., Jing, W. X., Fan, J. H., Li, D., et al. (2014a). Reduction of selenite to red elemental selenium by *RhodoPseudomonas palustris* strain N. *PLoS one.* 9:e95955. doi: 10.1371/journal.pone.0095955
- Li, D., Zhou, C. R., Zhang, J. B., An, Q. S., Wu, Y. L., Li, J. Q., et al. (2020). Nanoselenium foliar applications enhance the nutrient quality of pepper by activating the *capsaicinoid* synthetic pathway. *J. Agric. Food Chem.* 68, 9888–9895. doi: 10.1021/acs.jafc.0c03044
- Li, D. B., Cheng, Y. Y., Wu, C., Li, W. W., Li, N., Yang, Z. C., et al. (2014b). Selenite reduction by *Shewanella oneidensis* MR-1 is mediated by fumarate reductase in periplasm. *Sci. Rep.* 4, 1–7. doi: 10.1038/srep03735
- Li, J. H., Yang, W. P., Guo, A. N., Qi, Z. W., Chen, J., Huang, T. M., et al. (2021). Combined foliar and soil selenium fertilizer increased the grain yield, quality, total Se, and organic Se content in naked oats. *J. Cereal Sci.* 100:103265. doi: 10.1016/j.jcs.2021.103265
- Liu, C., Tan, L., Zhang, L. M., Tian, W. Q., and Ma, L. Q. (2021). A review of the distribution of antibiotics in water in different regions of China and

- current antibiotic degradation pathways. *Front. Env. Sci.Switz.* 9:62298. doi: 10.3389/fenvs.2021.692298
- Luo, H. W., Du, B., He, L. X., Zheng, A. X., Pan, S. G., and Tang, X. R. (2019). Foliar application of sodium selenate induces regulation in yield formation, grain quality characters and 2-acetyl-1-pyrroline biosynthesis in fragrant rice. *BMC Plant Biol.* 19, 1–12. doi: 10.1186/s12870-019-2104-4
- Oremland, R. S., Herbel, M. J., Blum, J. S., Langley, S., Beveridge, T. J., Ajayan, P. M., et al. (2004). Structural and spectral features of selenium nanospheres produced by Se-respiring bacteria. *Appl. Environ. Microbiol.* 70, 52–60. doi: 10.1128/AEM.70.1.52-60.2004
- Rani, A., Shouche, Y. S., and Goel, R. (2008). Declination of copper toxicity in pigeon pea and soil system by growth-promoting *Proteus vulgaris* KNP3 Strain. *Curr. Microbiol.* 57, 78–82. doi: 10.1007/s00284-008-9156-2
- Ruiz Fresneda, M. A., Delgado Martín, J., Gómez Bolívar, J., Fernández Cantos, M. V., Bosch-Estévez, G., Martínez Moreno, M. F., et al. (2018). Green synthesis and biotransformation of amorphous Se nanospheres to trigonal 1D Se nanostructures: impact on Se mobility within the concept of radioactive waste disposal. *Environ. Sci. Nano.* 5, 2103–2116. doi: 10.1039/C8EN00221E
- Shin, Y. S., Blackwood, J. M., Bae, I. T., Arey, B. W., and Exarhos, G. J. (2007). Synthesis and stabilization of selenium nanoparticles on cellulose nanocrystal. *Mater Lett.* 61, 4297–4300. doi: 10.1016/j.matlet.2007.01.091
- Song, D. G., Li, X. X., Cheng, Y. Z., Xiao, X., Lu, Z. Q., Wang, Y. Z., et al. (2017). Aerobic biogenesis of selenium nanoparticles by *Enterobacter cloacae* Z0206 as a consequence of fumarate reductase mediated selenite reduction. *Sci. Rep.* 7:3239. doi: 10.1038/s41598-017-03558-3
- Soudi, M., Ghazvini, P., Khajeh, K., and Gharavi, S. (2008). Bioprocessing of seleno-oxyanions and tellurite in a novel *Bacillus* sp strain STG-83: a solution to removal of toxic oxyanions in presence of nitrate. *J. Hazard. Mater.* 165, 71–77. doi: 10.1016/j.jhazmat.2008.09.065
- Tugarova, A. V., Mamchenkova, P. V., Dyatlova, Y. A., and Kamnev, A. A. (2018). FTIR and raman spectroscopic studies of selenium nanoparticles synthesized by the bacterium *Azospirillum thioophilum*. *Spectrochim. Acta Part A* 192, 458–463. doi: 10.1016/j.saa.2017.11.050
- Wang, Y. T., Shu, X., Hou, J. Y., Lu, W. L., Zhao, W. W., Huang, S. W., et al. (2018a). Selenium nanoparticle synthesized by *Proteus mirabilis* YC801: an efficacious pathway for selenite biotransformation and detoxification. *Int. J. Mol. Sci.* 19:3809. doi: 10.3390/ijms19123809
- Wang, Y. T., Shu, X., Zhou, Q., Fan, T., Wang, T. C., Chen, X., et al. (2018b). Selenite reduction and the biogenesis of selenium nanoparticles by *Alcaligenesfaecalis* Se03 isolated from the gut of *Monochamus alternatus* (Coleoptera: Cerambycidae). *Int. J. Mol. Sci.* 19:2799. doi: 10.3390/ijms19092799
- Xu, C. L., Qiao, L., Guo, Y., Ma, L., and Cheng, Y. Y. (2018). Preparation, characteristics and antioxidant activity of polysaccharides and proteins-capped selenium nanoparticles synthesized by *Lactobacillus casei* ATCC 393. *Carbohydr. Polym.* 195, 576–585. doi: 10.1016/j.carbpol.2018.04.110
- Yan, J., Chen, X. J., Zhu, T. G., Zhang, Z. P., and Fan, J. B. (2021). Effects of selenium fertilizer application on yield and selenium accumulation characteristics of different japonica rice varieties. *Sustainability* 13:10284. doi: 10.3390/su131810284
- Zahedi, S. M., Hosseini, M. S., Meybodi, N. D. H., Teixeira, and da Silva, J. A. (2019). Foliar application of selenium and nano-selenium affects pomegranate (*Punica granatum* cv. Malase Saveh) fruit yield and quality. *S. Afr. J. Bot.* 124, 350–358. doi: 10.1016/j.sajb.2019.05.019
- Zhang, H. Q., Zhao, Z. Q., Zhang, X., Zhang, W., Huang, L. Q., Zhang, Z. Z., et al. (2019a). Effects of foliar application of selenate and selenite at different growth stages on Selenium accumulation and speciation in potato (*Solanum tuberosum* L.). *Food Chem.* 286, 550–556. doi: 10.1016/j.foodchem.2019.01.185
- Zhang, J., Wang, Y., Shao, Z. Y., Li, J., Zan, S. T., Zhou, S. B., et al. (2019b). Two selenium tolerant *Lysinibacillus* sp. strains are capable of reducing selenite to elemental Se efficiently under aerobic conditions. *J. Environ. Sci.* 77, 238–249. doi: 10.1016/j.jes.2018.08.002
- Zhang, Y. Q., and Frankenberger, W. (2006). Removal of selenate in river and drainage waters by *Citrobacter braakii* enhanced with zero-valent iron. *J. Agric. Food Chem.* 54, 152–156. doi: 10.1021/jf058124o
- Zhang, Y. Q., and Frankenberger, W. (2007). Supplementing *Bacillus* sp. RS1 with *Dechloromonas* sp. HZ for enhancing selenate reduction in agricultural drainage water. *Sci. Total Environ.* 372, 397–405. doi: 10.1016/j.scitotenv.2006.10.027
- Zheng, S. X., Su, J., Wang, L., Yao, R., Wang, D., Deng, Y. J., et al. (2014). Selenite reduction by the obligate aerobic bacterium *Comamonas testosteroni* S44 isolated from a metal-contaminated soil. *BMC Microbiol.* 14:204. doi: 10.1186/s12866-014-0204-8
- Zhu, Y. Y., Ren, B. Y., Li, H. F., Lin, Z. Q., Bañuelos, G., Li, L., et al. (2018). Biosynthesis of selenium nanoparticles and effects of selenite, selenate, and selenomethionine on cell growth and morphology in *Rahnella aquatilis* HX2. *Appl. Microbiol. Biotechnol.* 102, 6191–6205. doi: 10.1007/s00253-018-9060-z
- Zonaro, E., Piacenza, E., Presentato, A., Monti, F., Dell'Anna, R., Lampis, S., et al. (2017). Ochrobactrum sp. MPV1 from a dump of roasted pyrites can be exploited as bacterial catalyst for the biogenesis of selenium and tellurium nanoparticles. *Microb. Cell Fact.* 16:215. doi: 10.1186/s12934-017-0826-2

**Conflict of Interest:** The authors declare that the research was conducted in the absence of any commercial or financial relationships that could be construed as a potential conflict of interest.

**Publisher's Note:** All claims expressed in this article are solely those of the authors and do not necessarily represent those of their affiliated organizations, or those of the publisher, the editors and the reviewers. Any product that may be evaluated in this article, or claim that may be made by its manufacturer, is not guaranteed or endorsed by the publisher.

Copyright © 2022 Huang, Jiang, Wang and Huang. This is an open-access article distributed under the terms of the Creative Commons Attribution License (CC BY). The use, distribution or reproduction in other forums is permitted, provided the original author(s) and the copyright owner(s) are credited and that the original publication in this journal is cited, in accordance with accepted academic practice. No use, distribution or reproduction is permitted which does not comply with these terms.